

TI Designs: TIDA-01465

电容式冰霜检测参考设计 - 分辨率小于 1mm, 温度漂移小于 0.25%



说明

在冰箱、空调和冷冻柜等电器应用中，冷却体和蒸发器上的冰霜堆积会导致系统能效大幅度降低。

该传感器参考设计通过减少非必要除霜周期的数量，帮助满足现代电器更严格的能效要求。该设计旨在通过感测冷却体外壳和金属表面的积冰量（精度小于 1mm），然后仅在必要时触发除霜周期，从而控制和确定除霜频率。该设计提供了使用计时器或温度传感器这一传统除霜触发方法的替代方案。

资源

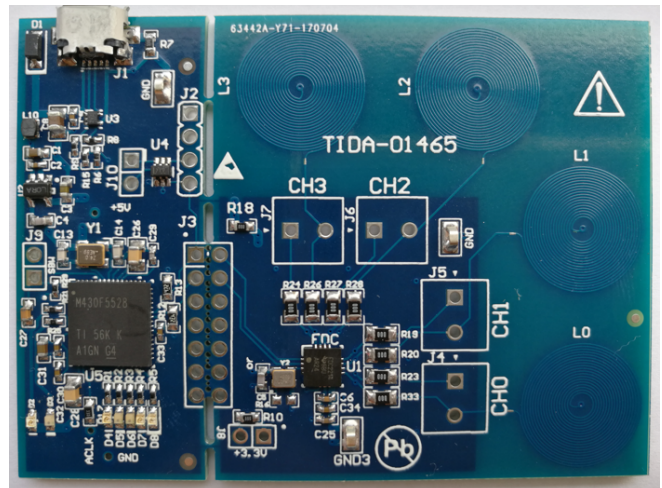
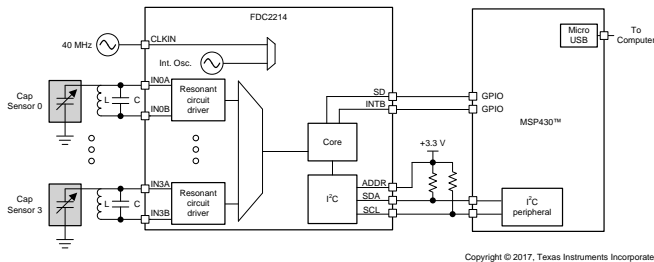
| | |
|-----------------------------|-------|
| TIDA-01465 | 设计文件夹 |
| FDC2214 | 产品文件夹 |
| MSP430F5528 | 产品文件夹 |
| LP2985-N | 产品文件夹 |
| TPD2E001 | 产品文件夹 |

特性

- 适用于各种制冷设备的通用应用，灵敏度高、可靠性高且成本低
- 支持多达四个通道的传感器
- 准确感测制冷设备蒸发线圈表面堆积的任何冰霜厚度
- 灵活控制制冷设备蒸发线圈表面的冰霜堆积
- 最大限度减少在蒸发器线圈上消融冰霜的除霜周期，省去不必要的除霜周期，节能省电
- 能够检测物质状态的物理变化
- 电容式传感技术具有基于窄带的创新架构，可在高速提供高分辨率的同时有效抑制噪声和干扰

应用

- 冰箱
- 空调
- 冷冻柜



该 TI 参考设计末尾的重要声明表述了授权使用、知识产权问题和其他重要的免责声明和信息。

1 System Description

The accumulation of ice or frost on an evaporator coil always presents a problem in modern refrigeration home appliances such as refrigerators, freezers, and air conditioners. The accumulation or buildup of ice or frost insulates the air to be cooled or refrigerated from the cold refrigerating fluid circulating through the evaporator unit, which makes maintaining the refrigerated space at the desired temperature difficult. Also, when atmospheric conditions that lead to the formation of ice on a cooling body arise, the heat exchange is blocked, which subsequently reduces the overall efficiency. Solving these problems requires a defrost system that is operatively associated with the heat exchanger of a cooling body. The question to address is when to activate the defrost cycle.

Previously used methods have offered several techniques to solve this problem. One conventional method that is widely used provides for a time clock, which at some preselected time interval shuts off the compressor and turns on a thermal heating device adjacent to the evaporator coils to melt the ice or frost. The disadvantage of this technique is that ice or frost does not always accumulate at a constant rate, depending on the ambient humidity and temperature of the air, and most clock-actuated defrost systems defrost more often than necessary as a cautionary measure to eliminate all buildup of ice or frost. This defrosting on a regular time cycle, whether necessary or not, does not consider the quantity of accumulated ice or frost, thereby causing inefficiency and wasting electrical power. Another method is to simply shut off the compressor for a predetermined length of time that is generally sufficient to allow the ice or frost to melt. However, this method is also inefficient because turning off the compressor permits the refrigerated space temperature to rise and continually makes the compressor and its motor work excessively to maintain the desired temperature. Other techniques use temperature-sensitive devices to measure the temperature of the refrigerating medium and signal the defrost cycle upon a predetermined rise in the temperature as detected by the device. These temperature-sensitive devices are generally inaccurate because they must be extremely sensitive to detect a small change in the temperature of the refrigerating medium, which corresponds to a wide variation in the thickness of ice or frost accumulation.

The most effective method is to sense the quantification of frost and ice buildup on the cooling body and initiate countermeasures at the proper time. Data about ice buildup can be useful to assist the activation of countermeasures. A controller, operatively coupled to the frost detection sensor or sensors and to the defrost system, selectively activates the defrost system to initiate a defrost cycle of the evaporator in response to the signal that indicates the presence of frost formation on the heat exchange tubes and heat transfer fins. This reference design demonstrates the direct capacitive measurement of frost formation, which improves defrost cycle control. The FDC2214 capacitive-to-digital converter from Texas Instruments enables the sensing of frost and ice. By mounting a capacitive sensor around the tube or fin of a cooling body, the system can sense the thickness of frost and ice by measuring the capacitance change between the sensor and tube/fin.

With this reference design, the consumer can get the benefit of:

- Boosting system energy efficiency
- Avoiding unnecessary disruptions of operation and defrost cycle
- Reducing unwanted audible noise

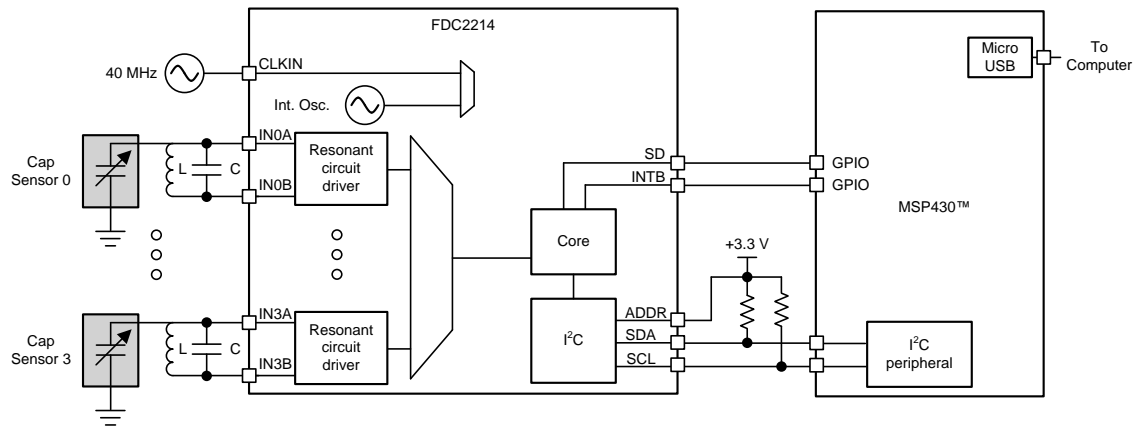
1.1 Key System Specifications

表 1. Key System Specifications

| PARAMETER | SPECIFICATIONS | DETAILS |
|------------------------|---------------------------------|-------------------------|
| Sensor type | Copper mesh sensor | 节 2.3.5 |
| Input voltage | 5-V nominal (VBUS from USB) | — |
| Sensitivity | Sensitivity resolution < 0.5 mm | 节 4.2.2 |
| Operating temperature | −40°C to 85°C | — |
| Self temperature drift | < 0.25% | 节 4.2.3 |
| Form factor | 70 mm × 51 mm | — |

2 System Overview

2.1 Block Diagram



Copyright © 2017, Texas Instruments Incorporated

图 1. TIDA-01465 System Block Diagram

2.2 Highlighted Products

The key part of this frost and ice detection reference design is the FDC2214, which uses capacitive sensing to detect the thickness of frost and ice. With an external MCU MSP430F5528, the user can easily set the parameters of the FDC2214 device and monitor the capacitance change curve through a graphical user interface (GUI) on a personal computer (PC). The following subsections detail the highlighted products used in this reference design, including the key features for their selection.

- **FDC2214**: Electromagnetic interference (EMI) resistant, 28-bit, capacitance-to-digital converter
- **MSP430F5528**: 16-bit, ultra-low-power microcontroller (MCU)
- **LP2985-N**: Micropower, 150-mA, low-noise ultra-low-dropout regulator
- **TPD2E001**: Low-capacitance, two-channel, ± 15 -kV electrostatic-discharge (ESD) protection array

See the respective product data sheet for complete details on any highlighted device on www.ti.com.

2.2.1 FDC2214

Capacitive sensing is a low-power, low-cost, high-resolution contactless sensing technique that can be applied to a variety of applications. The sensor in a capacitive sensing system is any metal or conductor, which allows for a low cost and highly-flexible system design. The main challenge that limits sensitivity in capacitive sensing applications is the noise susceptibility of the sensors.

The FDC2214 is a high-resolution, EMI-resistant, high-speed capacitance-to-digital multichannel converter for implementing capacitive sensing solutions. The devices employ an innovative narrowband-based architecture, L-C resonator, to offer high rejection of noise and interferers while providing high resolution at high speed. In contrast to traditional switched-capacitance architectures, the narrowband architecture allows unprecedented EMI immunity and a greatly-reduced noise floor. The devices support a wide excitation frequency range, offering flexibility in system design. With this innovative EMI resistant architecture, performance can be maintained even in presence of high-noise environments.

Using this approach, a change in capacitance of the L-C tank can be observed as a shift in the resonant frequency. Using this principle, the FDC2214 is a capacitance-to-digital converter (FDC) that measures the oscillation frequency of an LC resonator. The device outputs a digital value that is proportional to frequency. This frequency measurement can be converted to an equivalent capacitance.

Features:

- EMI-resistant architecture
- Maximum input capacitance: 250 nF (for a 10-kHz sensing system in any metal or conductor, permitting a 1-mH inductor)
- Sensor excitation frequency: 10 kHz to 10 MHz
- Number of channels: Four
- Resolution: Up to 28 bits
- Supply voltage: 2.7 V to 3.6 V
- Power consumption: Active, 2.1 mA
- Low-power sleep mode: 35 μ A
- Interface: I²C
- Temperature range: -40°C to $+125^{\circ}\text{C}$

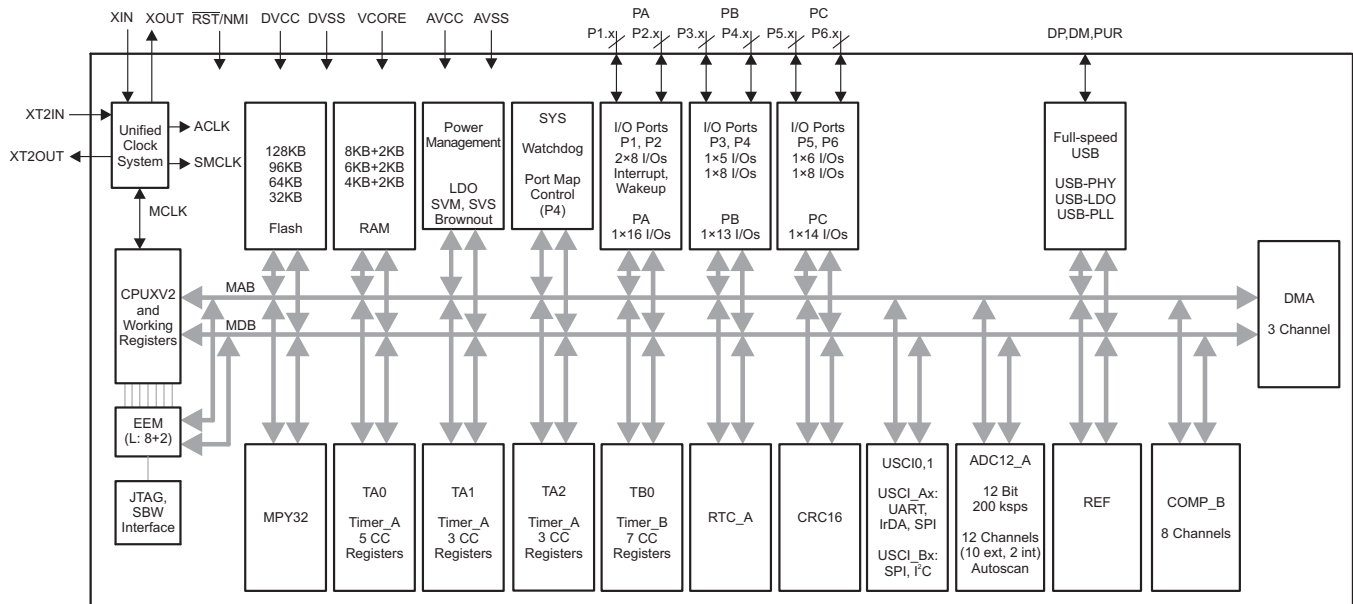
2.2.2 MSP430F5528

The TI MSP430™ family of ultra-low-power MCUs consists of several devices featuring peripheral sets targeted for a variety of applications. The architecture, combined with low-power modes, is optimized to achieve extended battery life in portable measurement applications. The MCU features a powerful 16-bit reduced instruction set computing (RISC) central processing unit (CPU), 16-bit registers, and constant generators that contribute to maximum code efficiency. The digitally controlled oscillator (DCO) allows the devices to wake up from low-power modes to activate in 3.5 μ s (typical).

With respect to MSP430F5528, the device has integrated USB and PHY, which supports USB 2.0, four 16-bit timers, a high-performance 12-bit analog-to-digital converter (ADC), two universal serial communication interfaces (USCI), a hardware multiplier, direct memory access (DMA), a real-time clock (RTC) module with alarm capabilities, and 47 input and output (I/O) pins.

Typical applications include analog and digital sensor systems, data loggers, and others that require connectivity to various USB hosts.

图 2 shows the functional block diagram of the MSP430F5528.



Copyright © 2017, Texas Instruments Incorporated

图 2. MSP430F5528 Functional Block Diagram

2.2.3 LP2985-N

The LP2985-N low-noise linear (LDO) regulator delivers up to 150-mA output current and only requires 300-mV dropout voltage of input to output. Using an optimized vertically-integrated PNP (VIP) process, the LP2985-N delivers unequalled performance for all low power consumption applications. The LP2985-N device provides 1% tolerance precision-output voltage with only 75- μ A quiescent current at a 1-mA load and 850 μ A at a 150-mA load. Reduce the output noise to 30 μ V_{RMS} in a 30-kHz bandwidth by adding a 10-nF bypass capacitor.

The LP2985-N is designed to work with a ceramic output capacitor with an equivalent series resistance (ESR) as low as 5 m Ω . The device is available with fixed output voltage from 2.5 V to 6.1 V.

图 3 shows the LP2985-N functional block diagram.

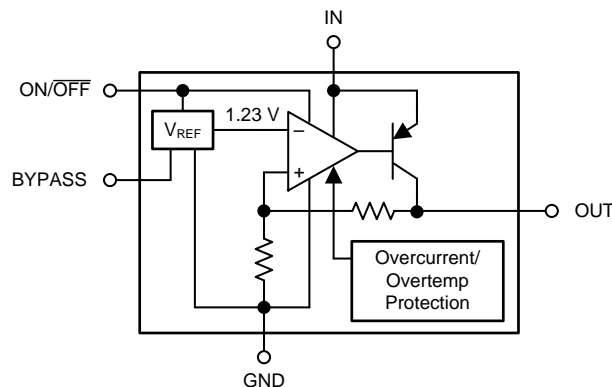


图 3. LP2985-N Functional Block Diagram

2.2.4 TPD2E001

The TPD2E001 is a two-channel transient voltage suppressor (TVS) based ESD protection diode array. The TPD2E001 is rated to dissipate ESD strikes at the maximum level specified in the IEC 61000-4-2 level 4 international standard. TI recommends to place one TVS for each channel of sensors.

图 4 shows the TPD2E001 typical USB application diagram.

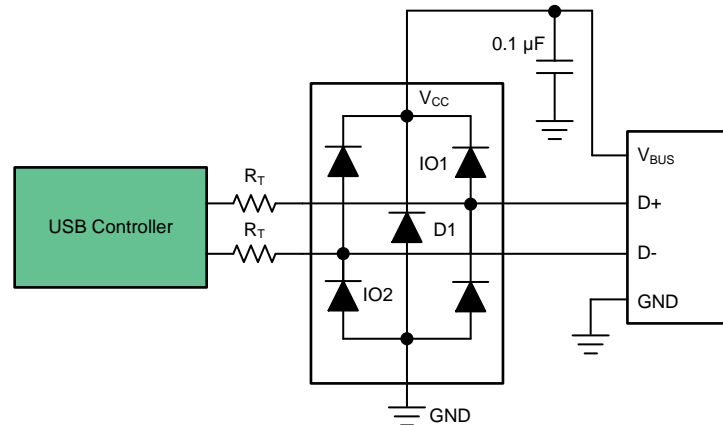


图 4. TPD2E001 Typical USB Application Diagram

2.3 System Design Theory

This reference design provides a solution for detecting the thickness of frost and ice accumulated on the surface of a cooling body using capacitive sensing technology from TI. The FDC2214 device measures the capacitance between the electrodes of a copper mesh sensor and the metal surface of a cooling body. The capacitance changes based on the thickness of frost or ice due to the variation of the dielectric constant between air and frost/ice.

2.3.1 Capacitance Measurement Basics

Capacitance is the ability of a capacitor to store an electrical charge. In a common form, such as a parallel plate capacitor, the capacitance is calculated by $C = Q / V$, where C is the capacitance related by the stored charge, Q , at a given voltage, V . The capacitance (measured in farads) of a parallel plate capacitor (see 图 5) consists of two conductor plates and is calculated using the following 公式 1:

$$C = \frac{\epsilon_r \times \epsilon_0 \times A}{d} \quad (1)$$

where,

- A is the area of the two plates (in meters),
- ϵ_r is the dielectric constant of the material between the plates,
- ϵ_0 is the permittivity of free space (8.85×10^{-12} F/m),
- d is the separation between the plates (in meters).

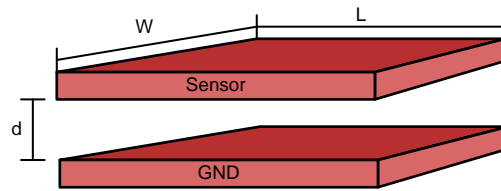


图 5. Parallel Plate Capacitor

The plates of a charged parallel plate capacitor carry an equal but opposite charge spread evenly over the surfaces of the plates. The electric field lines start from the charged plate with higher voltage potential and end at the charge plate with lower voltage potential. The parallel plate equation ignores the fringing effect due to the complexity of modeling the behavior; however, this formula is a good approximation if the distance (d) between the plates is small compared to the other dimensions of the plates so that the field in the capacitor is uniform over most of its area. The fringing effect occurs near the edges of the plates and, depending on the application, can affect the accuracy of measurements from the system. The density of the field lines in the fringe region is less than the density directly underneath the plates because the field strength is proportional to the density of the equipotential lines. This property results in weaker field strength in the fringe region and a much smaller contribution to the total measured capacitance. 图 6 shows the line paths of the electric fields of a parallel plate capacitor.

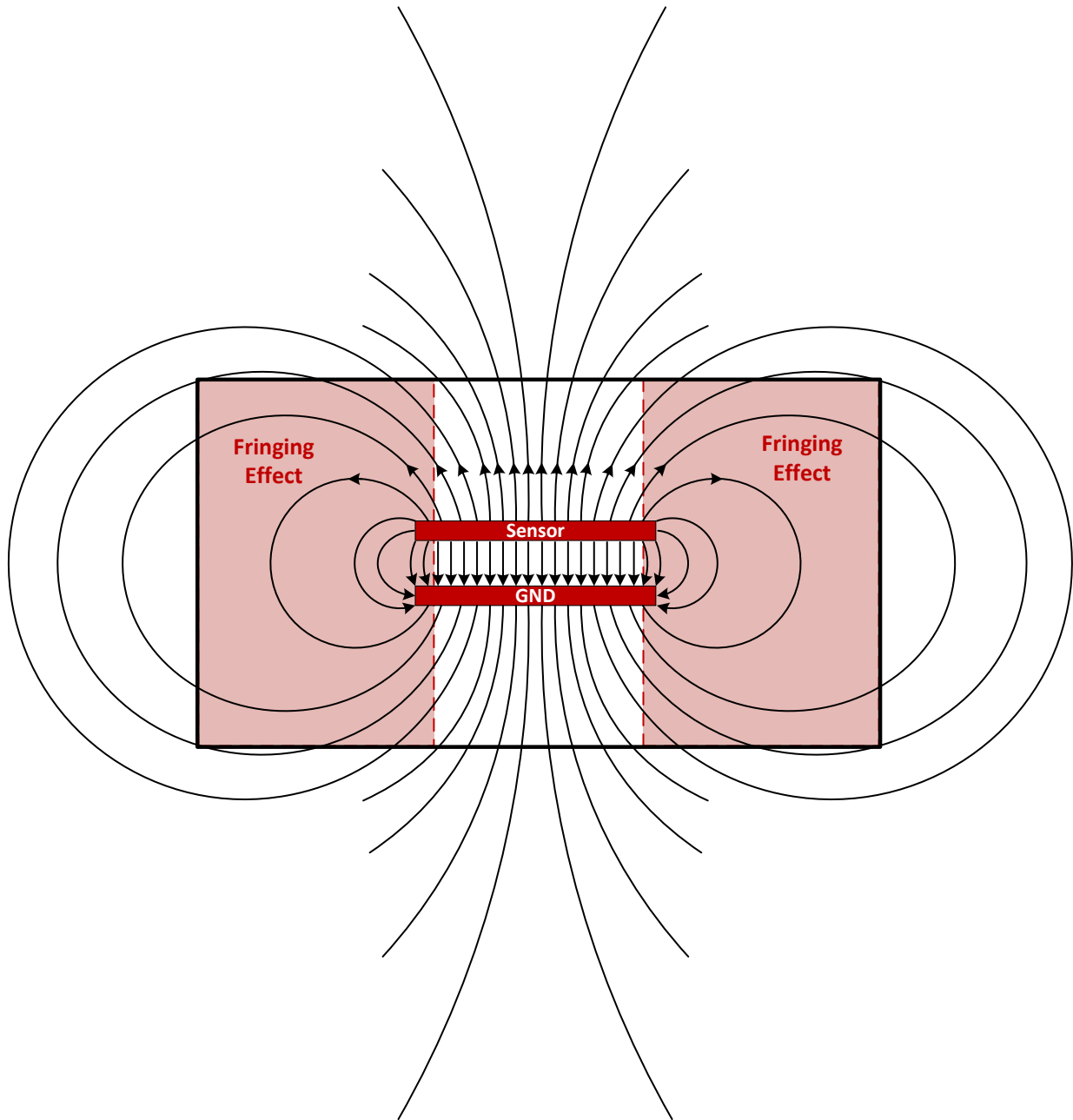


图 6. Electric Fields of Parallel Plate Capacitor

2.3.2 Capacitive Sensing

Capacitive sensing is a technology based on capacitive coupling. Capacitive sensing allows for a more reliable solution for applications to measure liquid levels, material composition, mechanical buttons, and human-to-machine interfaces (HMI). A basic capacitive sensor is anything that is metal or a conductor and detects anything that is conductive or has a dielectric constant different from the air. 图 7 shows three basic implementations for capacitive sensing: proximity or gesture recognition, liquid level sensing, and material analysis.

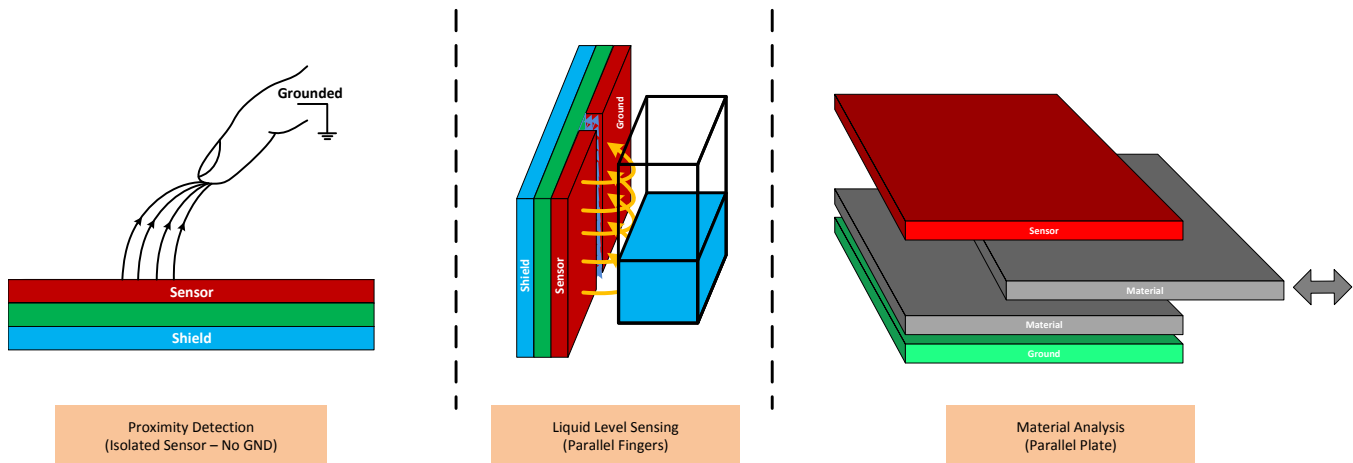


图 7. Basic Implements for Capacitive Sensing

Capacitance can be detected to sense different applications by changing one of the parameters while keeping the rest constant. For material analysis, the capacitance between the plates changes depending on the variation of dielectric constant from material to material. For paper stack height sensing, the capacitance increases as the number of sheets of paper are inserted between the plates. The difference between the air spacing and the paper spacing (due to the dielectric change and the known height of the paper and air spacing) allows the designer to calculate the capacitance. 表 2 shows the dielectric constant of some materials.

Quite similar to sensing paper stack height, the accumulation of frost and ice on the surface of a cooling body also causes the capacitance between two parallel plates (one is the metal surface of cooling body and the other is a specifically-designed sensor) to change due to the equivalent dielectric constant change, as 图 8 shows. When a properly-designed sensor composed of conducted material is fixed on the surface of a cooling body, the parameters for d , ϵ_0 , and A remain constant. Then the capacitance will be the function of equivalence of ϵ_r , which is the basic principle of this frost and ice detection reference design.

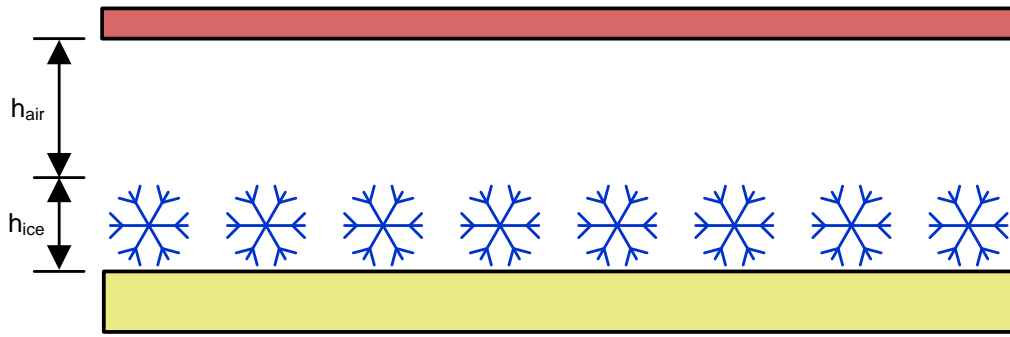


图 8. Model for Frost and Ice Detection Based on Capacitance

表 2 shows that ice has a dielectric constant three times that of air and an even greater dielectric constant than that of water. When ice and water are positioned near the parallel plate capacitor, the capacitance increases.

表 2. Material Dielectric Constants

| MATERIAL | DIELECTRIC CONSTANT (ϵ_r) | COMMENT |
|----------|--------------------------------------|---------|
| Air | 1 | — |
| Water | 80 | at 20°C |
| Glass | 7.6 to 8.0 | — |
| Paper | 2.3 | — |
| Ice | 3.2 | — |

2.3.3 Capacitive Sensing Circuit Design

In contrast to traditional switched-capacitance architectures, the FDC2214 employs an LC resonator, also known as an LC tank, as a sensor. The narrowband architecture allows unprecedented EMI immunity and greatly-reduced noise floor in comparison to other capacitive sensing solutions.

Using this approach, a change in capacitance of the LC tank can be observed as a shift in the resonant frequency. Using this principle, the FDC2214 is a capacitance-to-digital converter that measures the oscillation frequency of an LC resonator. The device outputs a digital value that is proportional to frequency and this frequency measurement can be converted to an equivalent capacitance.

图 9 shows the schematic of the capacitance detection circuits that contains the aforementioned LC tank. The combination of the L and C values determines the LC resonance frequency, as 公式 2 shows.

$$f = \frac{1}{2\pi\sqrt{LC}} \tag{2}$$

System-to-system variations in practical applications do exist and are mainly due to the component tolerances and environmental drift. The capacitors and the inductance of the coils are the main contributor to the system-to-system variation. TI recommends selecting high-quality capacitors such as the NP0/COG ceramic capacitors with a tolerance of 1%. This design uses double-layer printed-circuit board (PCB) coils instead of the commonly-used surface mount device (SMD) inductors due to their high temperature stability. Place the capacitors as close to the sensor coil as possible to reduce the parasitic inductance of the PCB traces.

The design value of L and C must meet the requirement of the FDC2214 (see [FDC2x1x EMI-Resistant 28-Bit, 12-Bit Capacitance-to-Digital Converter for Proximity and Level Sensing Applications \[1\]](#)) which specifies the oscillation frequency of the LC resonator in the range of 10 kHz to 10 MHz. For the PCB inductor in this design, each coil is 13.9 mm in diameter and contains 19 turns per layer. The nominal inductance is 8.6 μ H. The tank capacitor soldered in the PCB for each channel is a 39-pF, 1% ceramic NP0/COG SMD part. Also consider the additional pin, trace, and wire capacitance on the capacitive sensing circuit. Calculate the parasite capacitance by checking the FDC2214 conversion result, which the test results in 节 4.2.1 describe. With this design, the parasite capacitance of the board and wire is approximately 14.6 pF. The total capacitance in this reference design, which includes the tank capacitor (39 pF), parasitic capacitance (14.6 pF), and sensing capacitance, is approximately 70.7 pF and is observable in the GUI. These values make the tank oscillate at around 6.5 MHz nominally, which is below the 10-MHz operation limit. 节 4.1.2 shows the key parameters used in the GUI parameter settings.

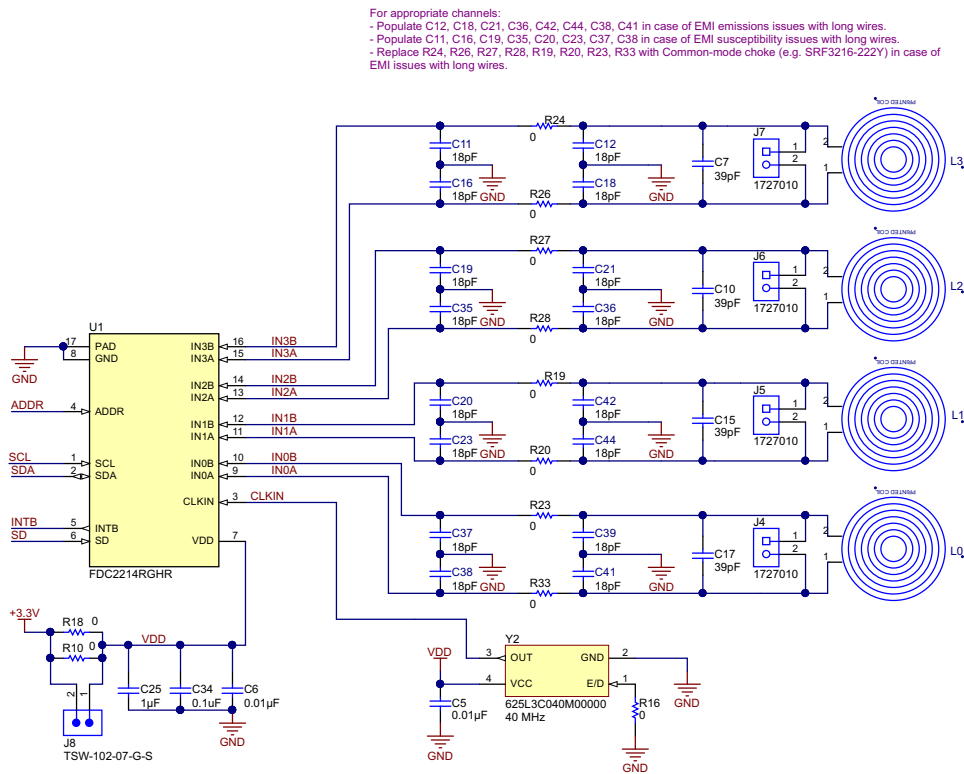


图 9. Schematic for Capacitance Detection Circuits

Increasing the capacitance value on the capacitive sensing circuit (C7, C10, C15, and C17) causes the static baseline capacitance to increase. This value increase improves the noise-to-baseline reference ratio and makes the system more robust to disturbances; however, this also reduces the sensitivity of the sensing circuit. Therefore, consider selecting the baseline capacitance during the design according to different application conditions.

The sensed capacitance may vary depending on the sensor size, distance of the sensing target, overlay material, and so forth. Typically, the sensor size is directly related to sensed capacitance. Bigger size means higher sensitivity. The sensor must be specifically designed based on the mechanical structure of the cooling body.

Therefore, one of the design challenges is the ratio between the capacitance sensed and the static capacitance of the system. Minimizing the static capacitance of the system is one of the most commonly considered solutions, but it is difficult to achieve due to the nature of the electronic components, the wire, and, sometimes, the frame of the end equipment.

The FDC2214 addresses this problem very nicely with 28 bits of high-resolution conversion results, which provide an accurate reading on small changes of the sensed capacitance.

The conversion value of the FDC2214 can be translated into capacitance using 公式 3:

$$C_{\text{SENSOR}} = \frac{1}{L \times (2\pi \times f_{\text{SENSOR}})^2} - C \tag{3}$$

where,

- C is the sum of the parallel sensor capacitance (capacitance of the LC tank) and parasitic capacitance.

The value for f_{SENSOR} is calculated using 公式 4:

$$f_{\text{SENSOR}} = \frac{\text{CH_FIN_SEL} \times f_{\text{REF}} \times \text{Count}}{2^{28}} \quad (4)$$

where,

- CH_FIN_SEL is the "sensor frequency select" bit value in the FDC2214 register, which is 1 in this design,
- f_{REF} is the reference frequency of the channel, which is 40 MHz in this design. If single mode is selected, the maximum value is 35 MHz.

Using the previous 公式 3 and 公式 4, translate the conversion result into capacitance.

Some components in the previous 图 9 schematic are optional and are used to enhance noise filtering when the circuit functions under harsh environment conditions (see *FDC2114 and FDC2214 EVM User's Guide* for more information [2]). TI also recommends utilizing ESD protection parts for sensor connection ports in any ESD sensitive applications.

2.3.4 Capacitive Sensor Topologies

Several capacitive sensor topologies exist that are common depending on the application. The sensor topology depends on:

- Sensor-to-target distance
- Dielectric constant of target
- Desired sensitivity

The basic topologies include:

- Parallel plate
- Parallel fingers
- Single sensor for human recognition

2.3.4.1 Parallel Plate

The parallel plate topology works exactly as described by the parallel plate capacitor equation in the previous 公式 1. The high density of electric fields between the two plates allows high sensitivity. Example applications for this topology are material analysis and sensing paper stack height, which 图 10 shows. For material analysis, the capacitance between the plates changes depending on the difference of the dielectric constant from material to material. The high resolution from the FDC2214 allows a sensitivity range that can detect very small changes in dielectric. When sensing paper stack height, the capacitance increases as the number of sheets of paper are inserted between the plates. The difference between the air spacing and the paper spacing (due to the dielectric change and the known height of the paper and air spacing) allows the capacitance to be calculated. This frost and ice detection reference design uses this topology and the basic principle from the material analysis also applies.

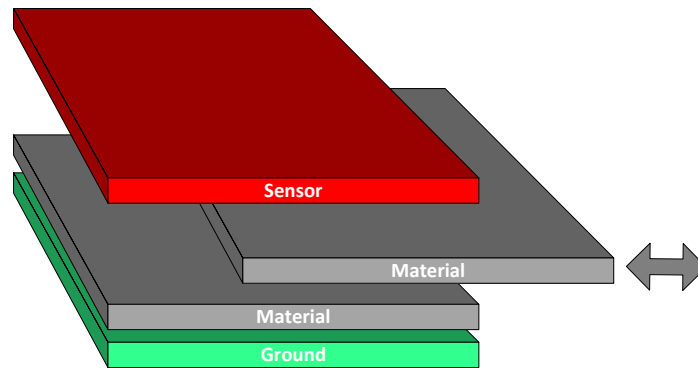


图 10. Parallel Plate Topology for Material Analysis

2.3.4.2 Parallel Fingers

The parallel fingers (GND sensor) topology works under the principle of fringing capacitance. High sensitivity along the z-axis (see 图 11) of the sensors enables the designer to implement this topology in liquid-level sensing applications. The electric field lines are more dominant near the edges between the sensor and ground plates. The capacitance calculations are not as straightforward as the simple parallel plate form but the sensitivity of the sensors increases as the sensor size increases (non-linearly). A shield on the backside of the main sensor and GND electrode provides directivity toward the target.

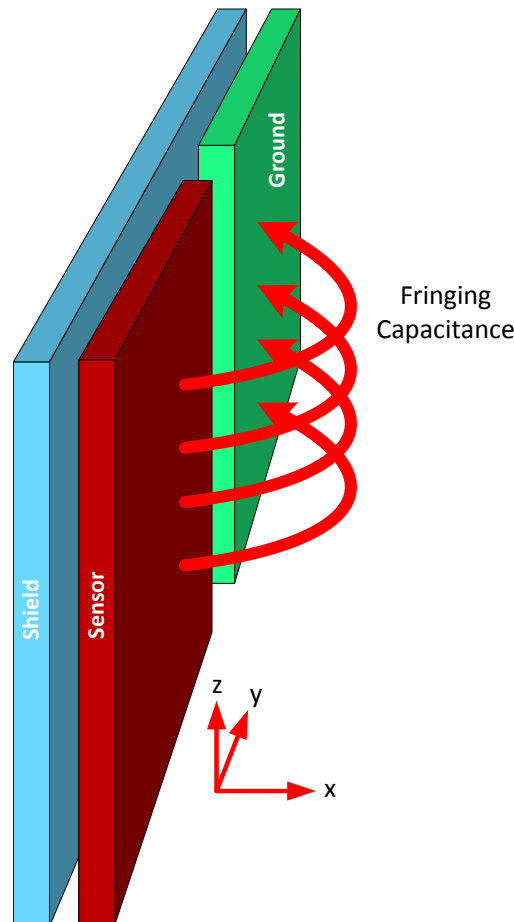


图 11. Parallel Fingers (GND Sensor) Topology

Several variant configurations can be designed with the parallel fingers. 图 12 shows the GND sensor configuration. Multiple sensor and ground electrodes can be alternated to have a central ground or sensor symmetry, as 图 12 shows. A central ground is required to establish a wide directivity along the width of the electrodes, which provides the widest response. A central sensor electrode is required to establish a high directivity along the width of the electrodes and provides the sharpest response. 图 13 shows the comb configuration which consists of both of these variants and is very effective for wide and high directivity. The comb configuration is typically for use in rain sensor applications and other applications that require a large sensing area and high sensitivity or resolution.

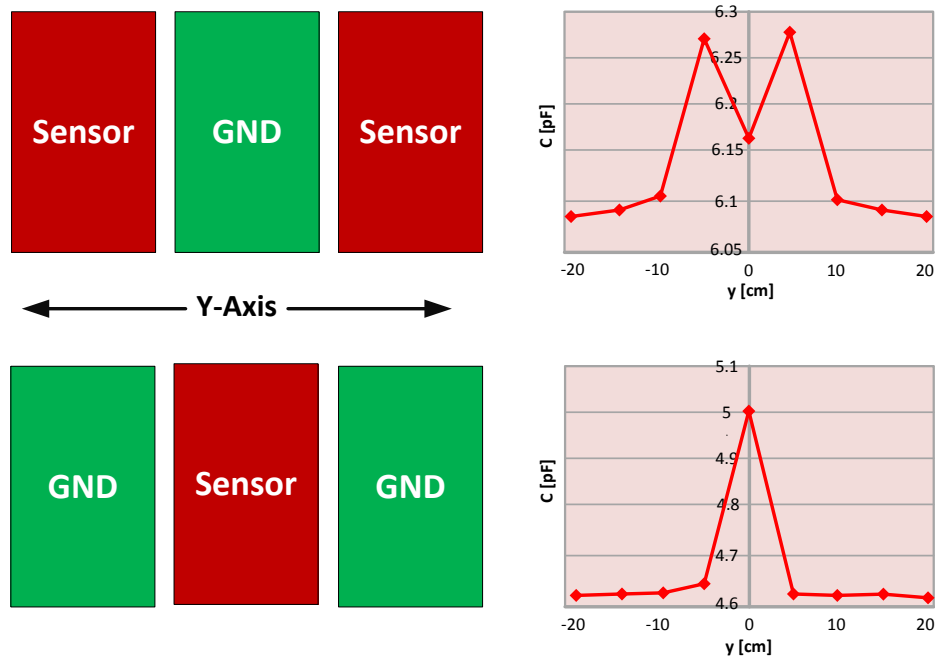


图 12. Central Ground, Central Sensor Symmetry

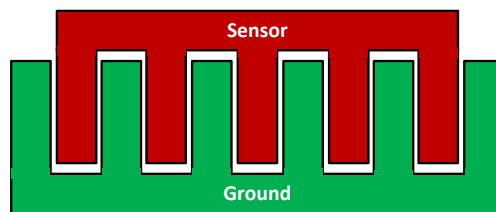


图 13. Comb Sensor Design

2.3.4.3 Single Sensor for Human Recognition

The single-sensor design for human recognition uses the same fringe capacitance principles as the parallel fingers topology except that the human hand or finger substitutes the ground electrode. Because the human body is grounded, the fringing electric field lines stray from the sensor to the hand as the hand approaches the sensor. This technique behaves similarly to the parallel plate equation because the distance between the sensor and GND (hand) electrodes is the only changing parameter. The capacitance increases as the hand moves closer to the sensor in a non-linear fashion because of fringing effects. The presence of the shield electrode underneath the sensor electrode helps reduce EMI and parasitic capacitances effects as 图 14 shows.

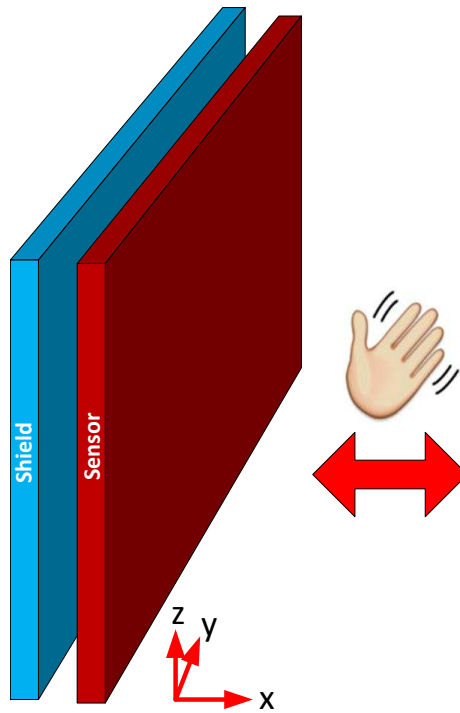


图 14. Single-Sensor Topology for Human Recognition

2.3.5 Sensor Design

When designing the sensor to detect frost and ice thickness, the topology of the parallel plate is chosen based on the descriptions provided in 节 2.3.4.1, 节 2.3.4.2, and 节 2.3.4.3.

As the previous 公式 1 shows, the sensor capacitance has a direct correlation with the area of the plates of the capacitor. An increase in the area of the sensor means an increase in the sensitivity. In this design, the target metal surface of a cooling body is one of the plates of a capacitor. The other target metal surface is a sensor which is specifically designed based on the mechanical structure of the cooling body.

图 15 shows two types of typical cooling bodies for a refrigerator or freezer.

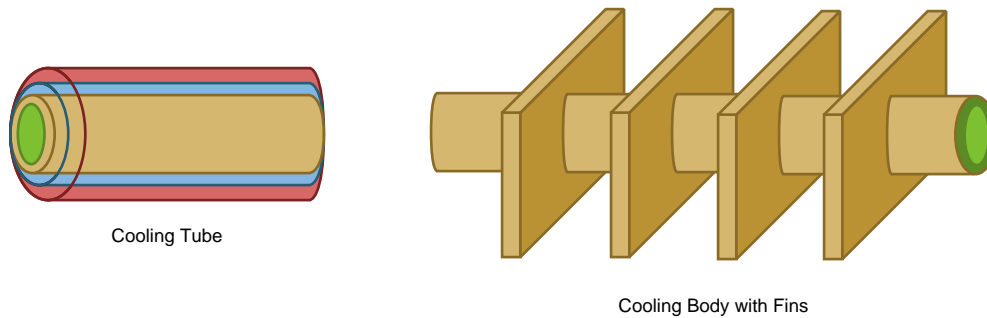


图 15. Cooling Body in Refrigerator or Freezer

图 16 shows the two types of sensor designs based on the structure of such cooling bodies.

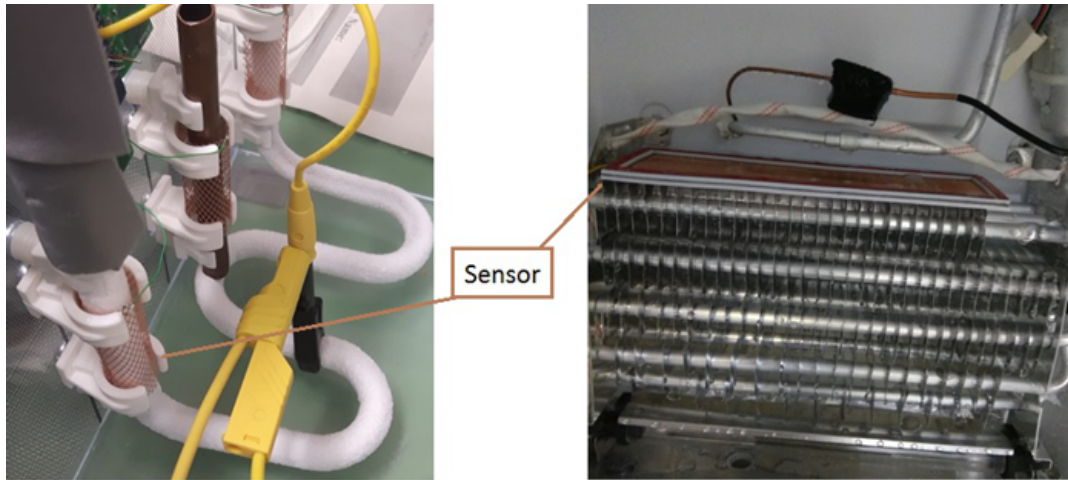


图 16. Capacitive Sensor

The first one-sensor design is fit for a cylindrical cooling tube and mounted around its surface. The second one-sensor design is specifically for a cooling body full of heat sink fins that have a flat edge surface. Copper mesh is selected for the material. The following 节 2.3.6 describes the key concerns for the sensor design.

图 17 shows an example of the expected capacitance change curve in principle. During stage 1, the capacitance remains a constant value when there is no frost and ice on the dry surface of the cooling body. From the very beginning of stage 2, the compressor of the refrigerator or air conditioner starts to work and the frost or ice gradually accumulates on the surface of the cooling body. Due to the dielectric constant change from air to ice (see 表 2), the capacitance increases based on the thickness of the frost or ice. The defrost cycle activates when the desired thickness has been detected. The capacitance experiences a sharp change when snow ($\epsilon_r = 3.2$) turns to water ($\epsilon_r = 80$), which stage 3 shows, and then returns back to the original value after the water drops from the cooling body.

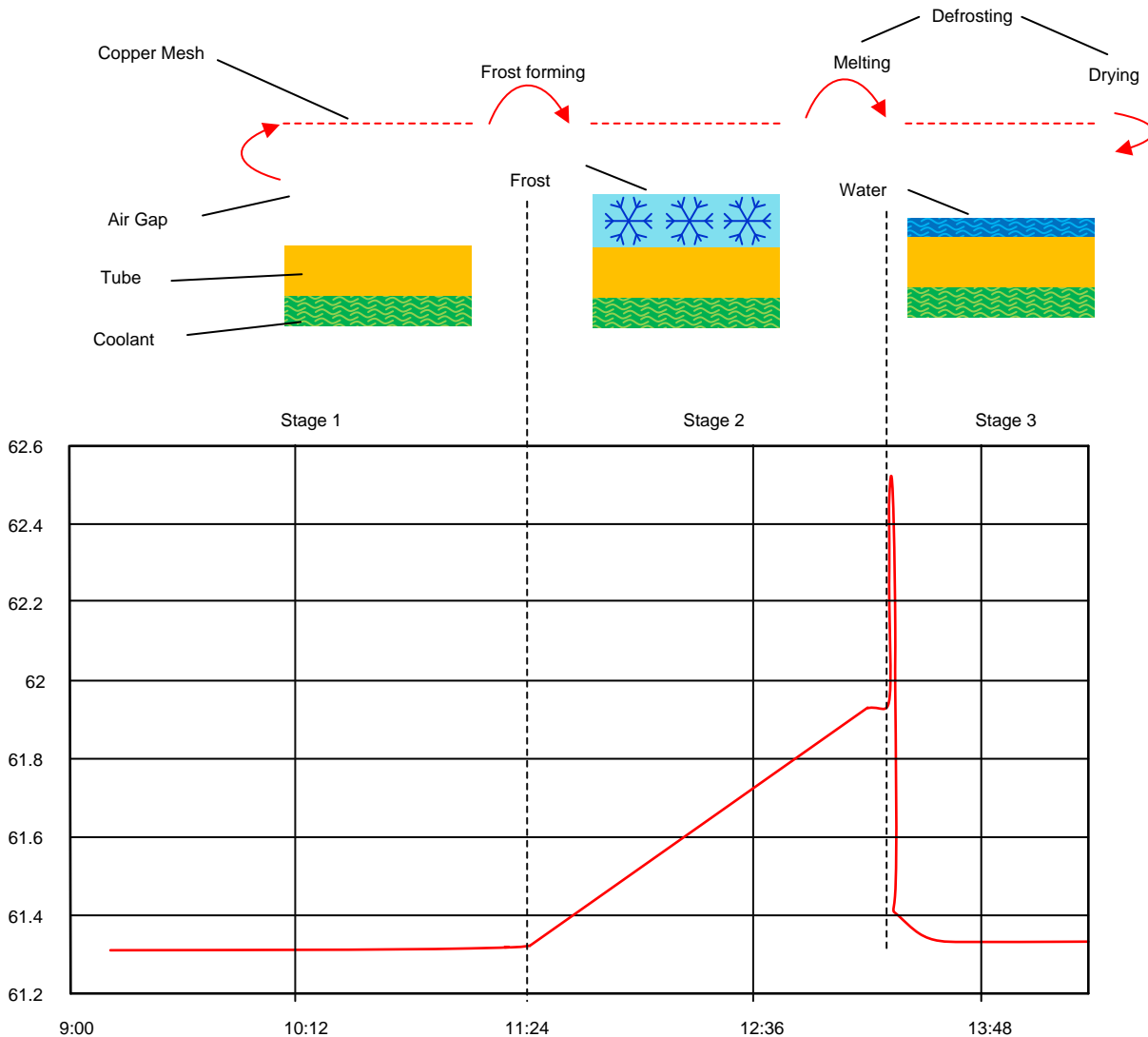


图 17. Capacitance Change in Single Cycle

2.3.6 Sensor Design Considerations

The space between the sensor electrode and cooling body forms sensor capacitor C_{SENSOR} . When designing the sensor portion, consider the size of the sensor electrodes, the coupling between the electrodes, and the cooling body. Follow these guidelines to ensure the maximum performance from the sensor system:

1. Maximize the ratio $C_{\text{SENSOR}} / C_{\text{PARASITIC}}$. As 图 18 shows:
 - A. Increase C_{SENSOR} by maximizing the ratio of sensor area A_{SENSOR} to distance d_{SENSOR} between the cooling body and sensor electrode.
 - B. Limit d_{SENSOR} close to the expected d_{FROSTMAX} , which is the maximum frost or ice thickness, to keep the margin as small as possible.
 - C. Minimize changing or drifting parasitic capacitances:
 1. Maximize the spacing of any objects changing position.
 2. Use the preferred unshielded, short cables for sensor connection unless they are required for signal integrity or to shield proximity events.

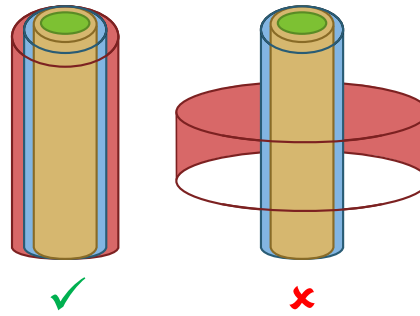


图 18. Sensor Optimization

 2. Target the proper C_{SENSOR} value. To do so:

1. Target a reasonable capacitance to achieve a suitable resonance frequency: < 8 MHz with a PCB coil of 8.6 μH .
2. Ensure the change of parasitic capacitance contributions (as the FDC input capacitance) are negligible versus the change in sensor capacitance resulting from ice formation.
TI recommends the following settings for a solid performance:

$$\Delta C_{\text{SENSOR}} > 0.5 \text{ pF} \Leftrightarrow C_{\text{sensor}} > 5 \text{ pF} \quad (5)$$

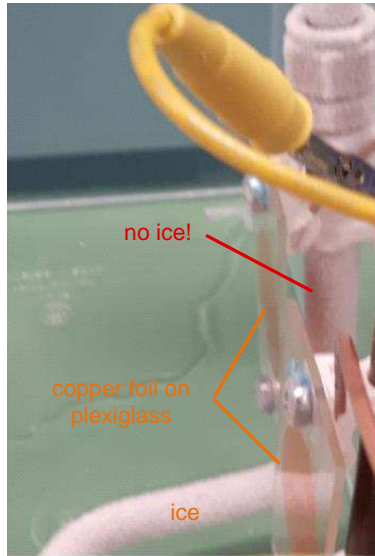
$$C_{\text{total}} = C_{\text{sensor}} + C_{\text{parasitic}} + C_{\text{tune}} > 60 \text{ pF} \quad (6)$$

注: Be sure to adjust the FDC internal filter frequency above the maximum oscillation frequency.

3. Guarantee a free airflow, equal ice formation, and full cooling capability.

Care is recommended in a sensor electrode design to ensure unimpeded free air flow (see 图 19). An unimpeded air flow encourages equal ice formation on the cooling body and allows for significant changes to capacitance in the sensing area. TI strongly recommends using a meshed electrode in the airflow. The designer can alternatively attach plates or foils to any plastic wall of the appliance housing if these do not interfere with the free airflow.

solid electrode impedes airflow



grid electrode free airflow

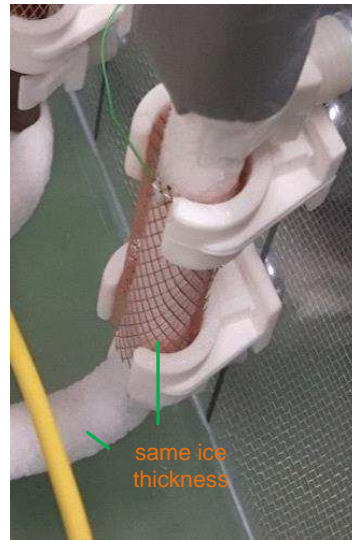


图 19. Different Ice Formation

4. Minimize presence of dew and drops around sensor the sensor.

Any presence of water in the sensing area causes a significant capacitance increase. Therefore, avoiding the accumulation of water in this area is critical. Water can be trapped due to surface tension on the electrodes, their fixtures, and tubes or fins of the cooling body. Avoid water accumulation through the means of vertical orientation, keeping out of the path of gravity, implementing a provision for an escape path for any water film or drops of sensor electrodes, and blowing some wind into the cooling body (see 图 20).

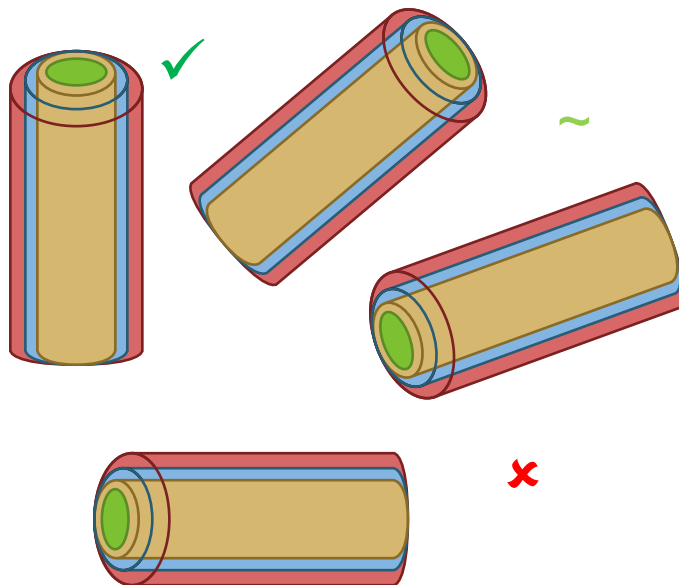


图 20. Different Orientations

5. Ensure a low impedance connection between sensor and resonance circuit.

The resonance frequency and measured capacitance depends to some degree on the resistance and proper damping of the resonance circuit. Constant resistance is better for ideal damping characteristic and good performance. TI strongly recommends to fabricate the sensor electrode from a single copper or metal plate to avoid the undefined contact resistance of loose wire meshes. Stamping and stretching guarantees both negligible airflow resistance and low ohmic resistance.

6. Ensure constant geometry and a solid fixture.
7. Avoid corrosion.

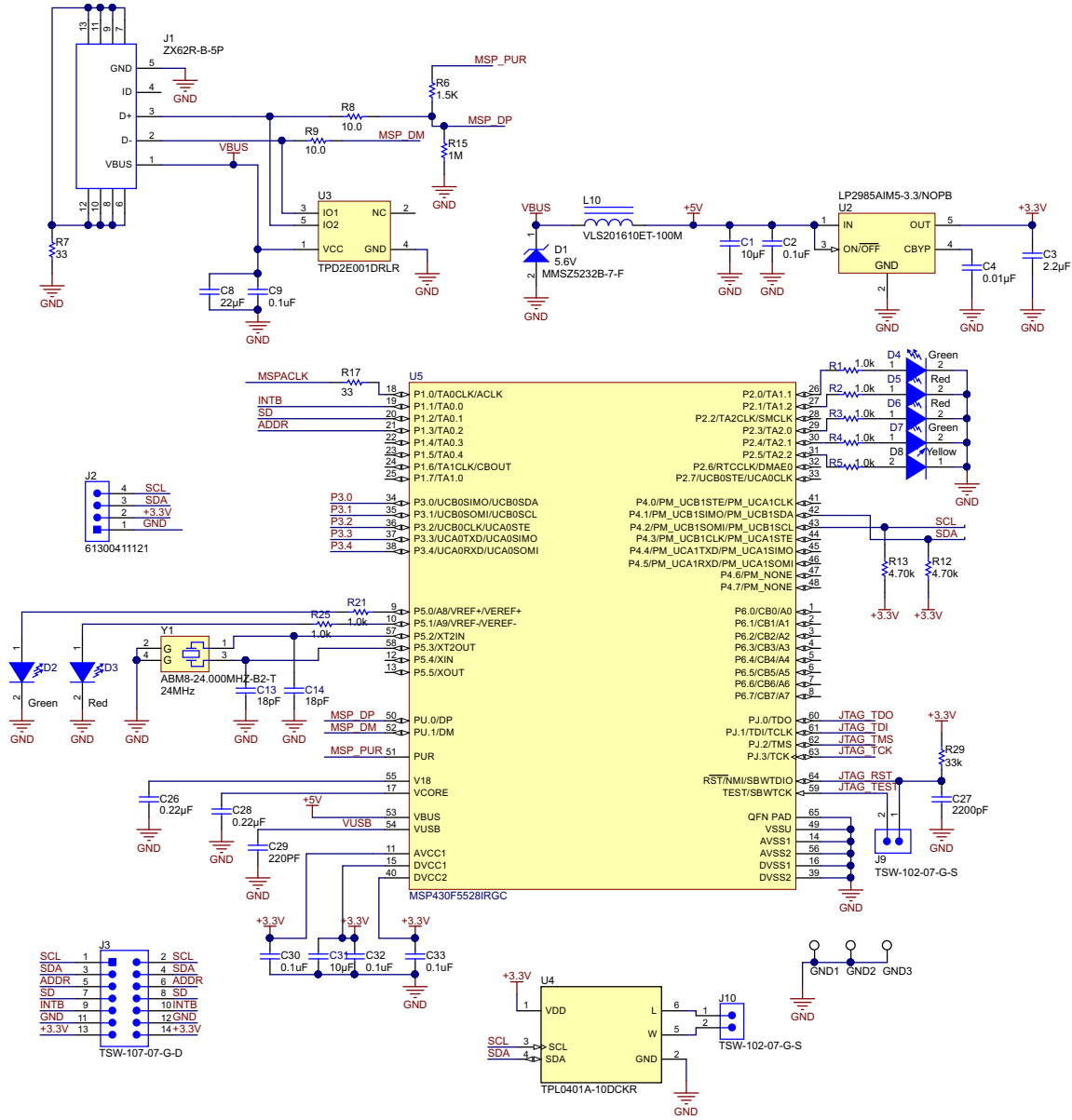
TI recommends to coat the sensor electrode to prevent corrosion.

8. Calibrate the sensor.

The initial errors in sensing systems originate from mechanical tolerance, coil inductance tolerance, capacitor tolerance, surrounding metals, and so forth. Calibration can greatly reduce the sensing errors caused by these initial tolerance errors. Calibration is generally performed prior to using the system. The calibration process generates data which is then stored permanently in the system. During use, the data-processing algorithm uses the calibration data to eliminate sensing error.

2.3.7 Removable Microcontroller Board

For FDC2214 output, use the I²C interface to support device configuration and to transmit the digitized frequency values to a host processor. This reference design uses a custom-designed auxiliary board (see 图 21) to communicate with a host computer and is controlled by an MSP430™ MCU. PCB perforations allow separation of the auxiliary board and the designer can connect alternative MCUs to the sensing board if desired.



Copyright © 2017, Texas Instruments Incorporated

图 21. Schematic for Auxiliary Control Board

3 Getting Started Hardware

This section describes the hardware overview and interface connector definitions in detail

3.1 Hardware Overview

图 22 shows the top view and bottom view of the PCB for the TIDA-01465 design. The board consists of two parts, one on each side. The left part is an auxiliary controller board which shows the capacitance change curve to the user through the GUI. The user can easily remove this auxiliary controller and connect the sensing board to their own system. The right part is the capacitance sensing and must connect to the sensor.

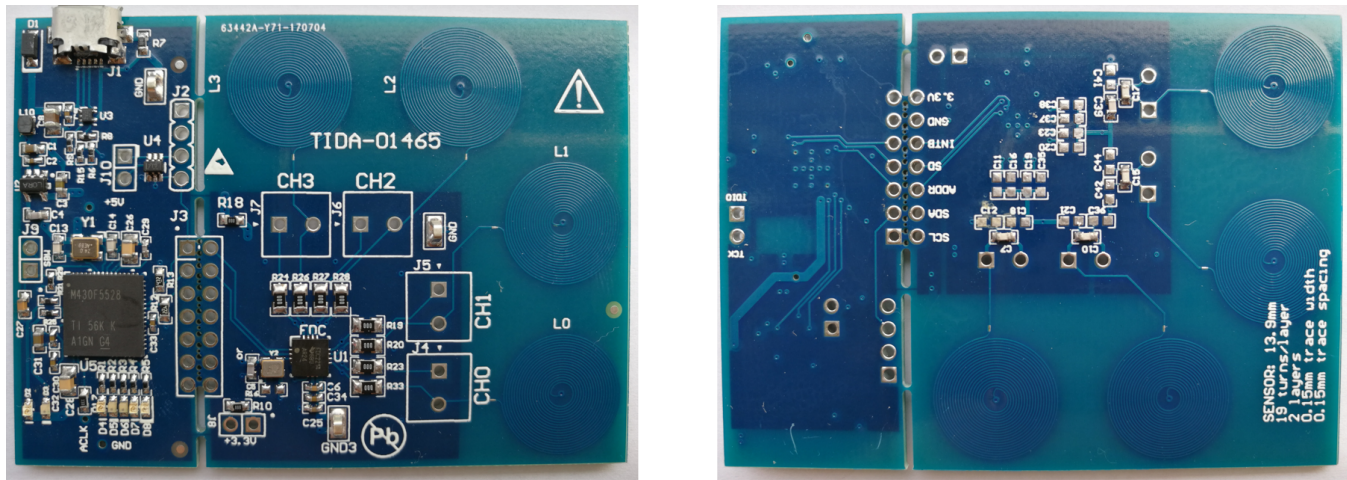


图 22. TIDA-01465 PCB—Top View and Bottom View

3.1.1 Connector Definitions

表 3. Connector Definitions

| PIN NUMBER | CH1/2/3/4 DEFINITION | J8 | J2 | J10 | J9 |
|------------|------------------------------|--------------------|-------|------------------|--------------------------|
| 1 | Custom Sensor ⁽¹⁾ | VDD ⁽²⁾ | GND | L ⁽³⁾ | JTAG_RST ⁽⁴⁾ |
| 2 | Custom Sensor ⁽¹⁾ | +3.3V | +3.3V | W ⁽³⁾ | JTAG_TEST ⁽⁴⁾ |
| 3 | — | — | SDA | — | — |
| 4 | — | — | SCL | — | — |

- ⁽¹⁾ Four channels can be selected: CH1, CH2, CH3, and CH4. For each channel, the custom sensor can be connected to one pin (either pin 1 or pin 2) of the connector while keeping the other one empty.
- ⁽²⁾ VDD is the power supply for FDC2214 and is short circuited to +3.3V by a 0-Ω resistor.
- ⁽³⁾ J10 outputs an adjustable analog signal which can be used to simulate NTC temperature sensing in the cooling system.
- ⁽⁴⁾ J9 is reserved for MCU programming.

4 Testing and Results

4.1 Test Setup

This section describes in detail the materials which are used for testing in the lab and how to set up the test platform step by step. Temperature and other interference testing has also been performed to verify how the reference design acts in different environments.

4.1.1 Materials to Prepare

Testing the performance of the reference design board and sensor for frost and ice detection requires some materials and equipment for preparation. 表 4 lists the materials required for the test setup and their basic usage.

表 4. Material Preparation

| MATERIALS | USAGE |
|---------------------|--|
| Refrigerator | Simulate the frost and ice forming on the surface of cooling body of refrigerator evaporator |
| Laptop | Continuously capture measurement data |
| Humidifier | Accelerate the frost and ice formation |
| Sensors | Sense the thickness of frost based on capacitive tech |
| TIDA-01465 board | Detect the capacitance value |
| Temperature chamber | Test the temperature drift of board |

4.1.2 Test Setup Procedure

The following steps show how to set up the test platform in the lab during the test.

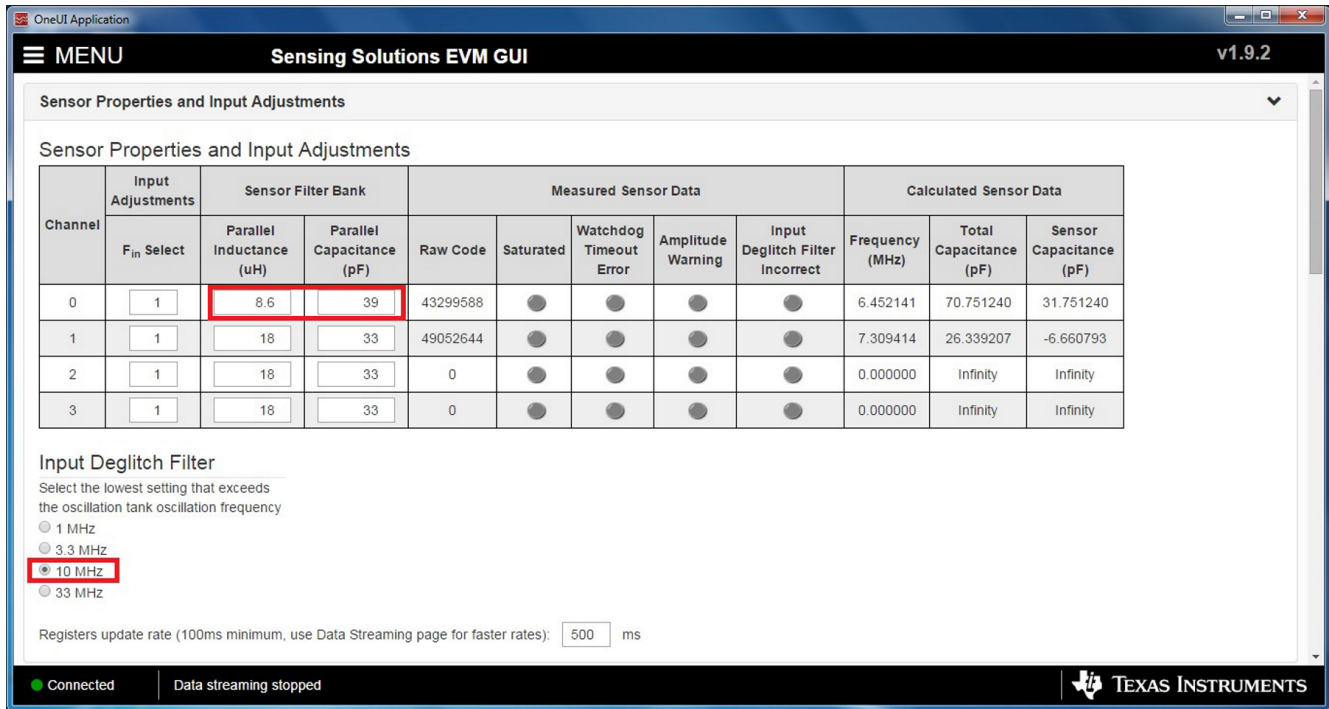
1. Make preparations for the refrigerator
 1. Switch off the power and open the freezing chamber.
 2. Remove the plastic parts in front of the evaporator.
 3. Expose the cooling body as 图 23 shows.
 4. Ensure that the cooling mechanism is functional with an open or partly-open door. An open door helps to allow sufficient humidity in for frost accumulation and also allows the user to more easily view the process.



图 23. Evaporator In Refrigerator

2. Make preparations for the laptop.
 1. Download [FDC2114 and FDC2214 EVM User's Guide \[2\]](#) and read it carefully.
 2. Make sure that the Microsoft® Windows® operating system installed in the laptop is 64-bit Windows 7 or 64-bit Windows XP.
 3. Request and download the [Sensing Solutions EVM GUI Tool v1.9.2 \(Rev. C\)](#) software and install it to the laptop.
 4. Make sure that the driver has also been installed in parallel; if not, the connection to the EVM will fail.

3. Affix the copper mesh sensor to the top surface of the cooling body and connect it to the TIDA-01465 board. Make sure that the board ground is connected to the metal part of the cooling body.
4. Attach the TIDA-01465 board to the computer through a micro USB cable.
5. Check the connection status on the bottom left corner of the GUI to make sure the connection is successful.
6. Adjusting certain parameters in the Sensing Solutions EVM GUI Tool v1.9.2 is important for obtaining the best performance using the TIDA-01465 design. Set the parameters as 图 24 shows.



Sensing Solutions EVM GUI v1.9.2

Sensor Properties and Input Adjustments

| Channel | Input Adjustments | Sensor Filter Bank | | Measured Sensor Data | | | | | Calculated Sensor Data | | |
|---------|------------------------|--------------------------|---------------------------|----------------------|-----------|------------------------|-------------------|---------------------------------|------------------------|------------------------|-------------------------|
| | F _{in} Select | Parallel Inductance (uH) | Parallel Capacitance (pF) | Raw Code | Saturated | Watchdog Timeout Error | Amplitude Warning | Input Deglitch Filter Incorrect | Frequency (MHz) | Total Capacitance (pF) | Sensor Capacitance (pF) |
| 0 | 1 | 8.6 | 39 | 43299568 | ● | ● | ● | ● | 6.452141 | 70.751240 | 31.751240 |
| 1 | 1 | 18 | 33 | 49052644 | ● | ● | ● | ● | 7.309414 | 26.339207 | -6.660793 |
| 2 | 1 | 18 | 33 | 0 | ● | ● | ● | ● | 0.000000 | Infinity | Infinity |
| 3 | 1 | 18 | 33 | 0 | ● | ● | ● | ● | 0.000000 | Infinity | Infinity |

Input Deglitch Filter
 Select the lowest setting that exceeds the oscillation tank oscillation frequency

1 MHz
 3.3 MHz
 10 MHz
 33 MHz

Registers update rate (100ms minimum, use Data Streaming page for faster rates): 500 ms

Connected | Data streaming stopped

图 24. Parameter Settings

7. Power on the refrigerator and activate the freezing cycle.
8. Monitor the capacitance change according to the thickness of frost and ice.

图 25 shows the final test setup.

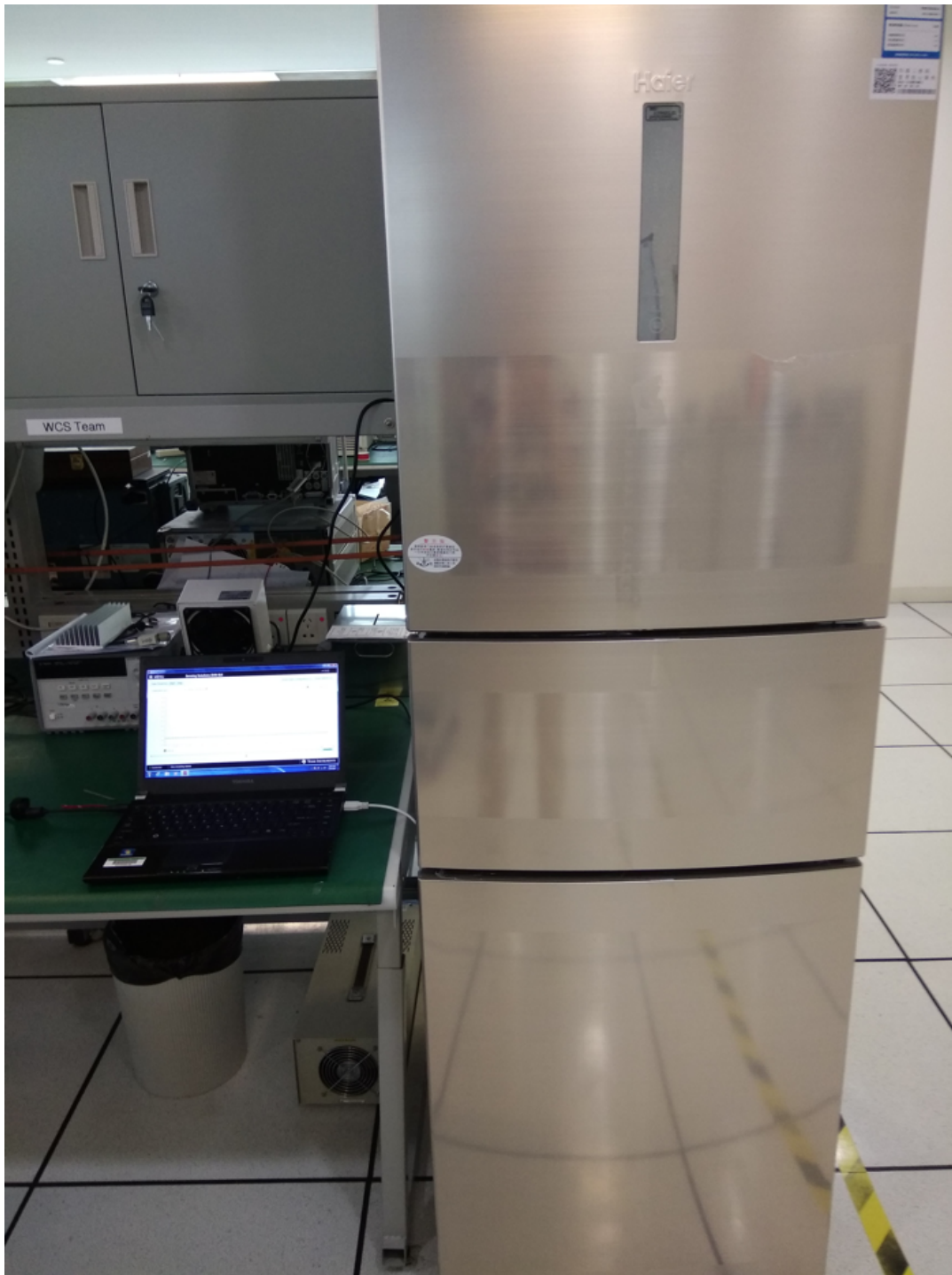


图 25. Test Setup Photo

4.2 Test Results

The test results of this reference design are divided in multiple sections that cover the capacitance repeatability with respect to the position, single cycle test, environmental susceptibility, temperature drift test, multi-cycle repeatability test, test influence of a 1.5-m cable connection, and conducted long-term drift test over one week.

4.2.1 Capacitance Repeatability With Respect to Position

This test aims to verify the repeatability of capacitance after placing the sensor in a different position on the cooling body. Due to the non-symmetry of an evaporator, the capacitance varies with respect to the position of the sensor. However, when the sensor is fixed in one position, the capacitance tolerance should be limited during the repeatability test. 图 26 和 图 27 显示测试设置和结果。

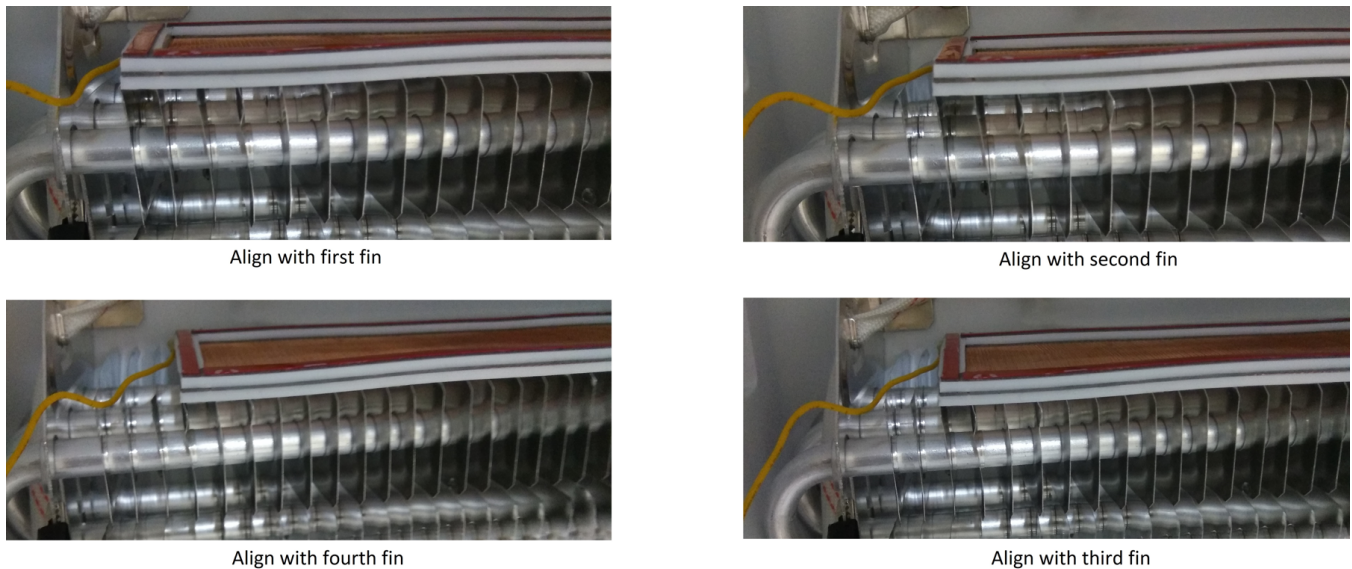


图 26. Capacitance Repeatability With Respect to Position

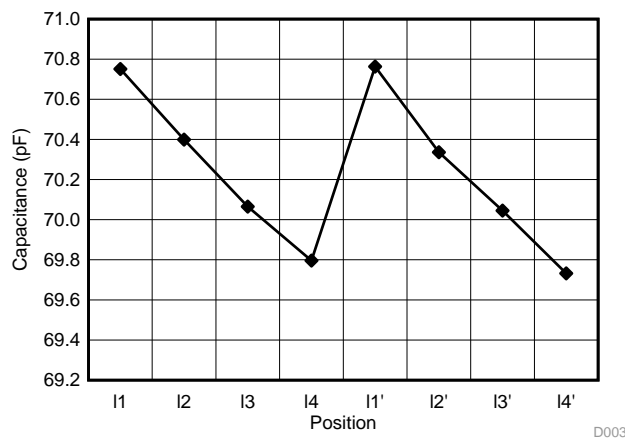


图 27. Capacitance Variation

4.2.2 Single Cycle Test

图 28 展示了在一个霜冻和冰形成及解冻周期中的电容变化。如图 28、图 29 和图 30 所示，电容与霜和冰的厚度成正比。当解冻周期启动时，电容值在很短的时间内急剧增加，这是因为介电常数从冰 ($\epsilon_r = 3.2$) 变为水 ($\epsilon_r = 80$)，然后在水从冷却体滴落后回到其原始值。

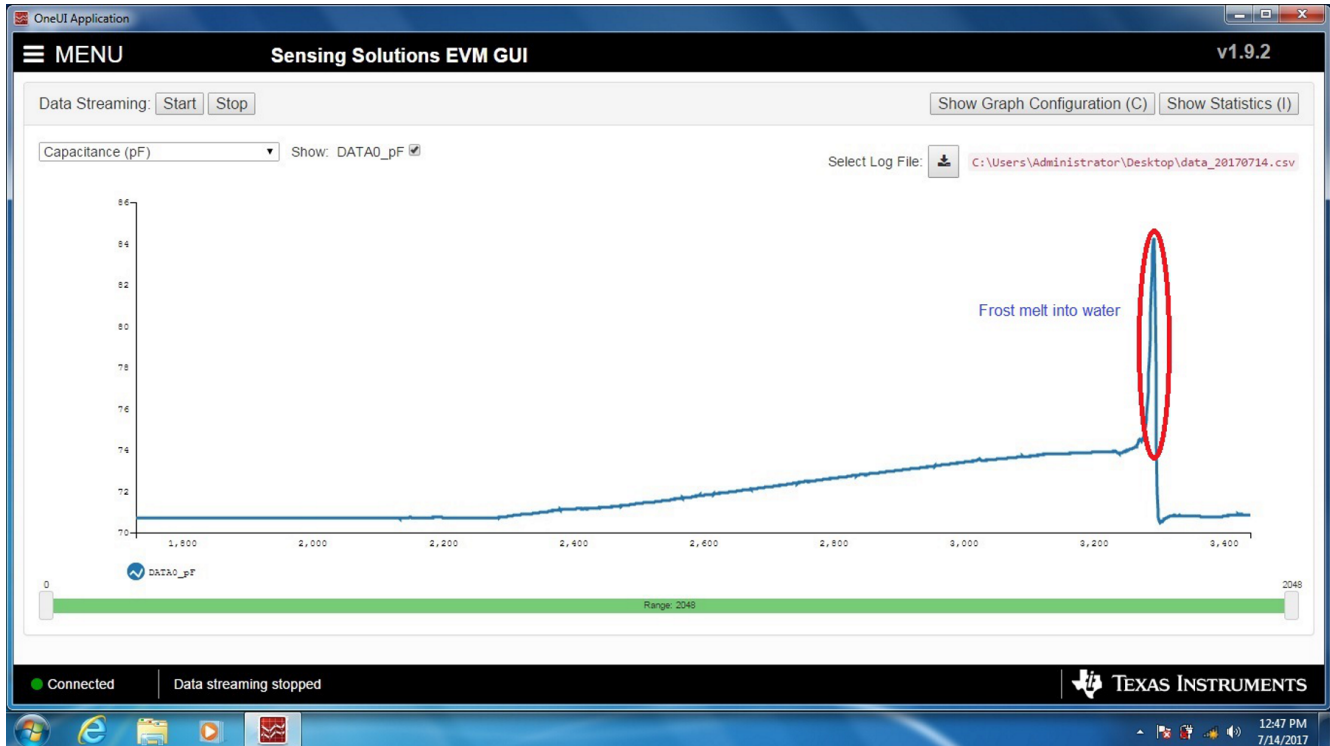
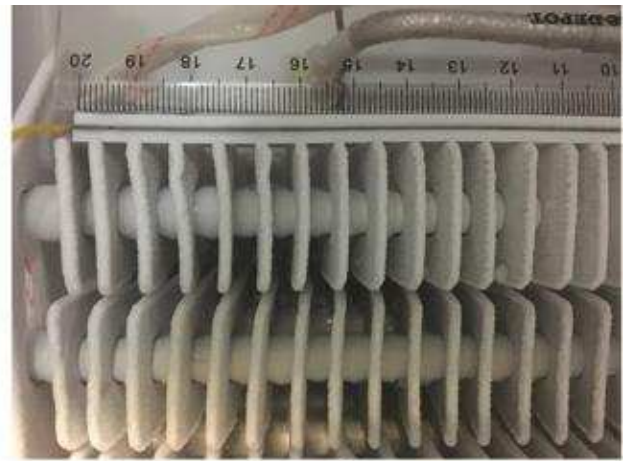


图 28. Single Cycle Test Overview

图 29 显示了六个具有不同霜和冰厚度的点。图 30 显示了相应的电容值。



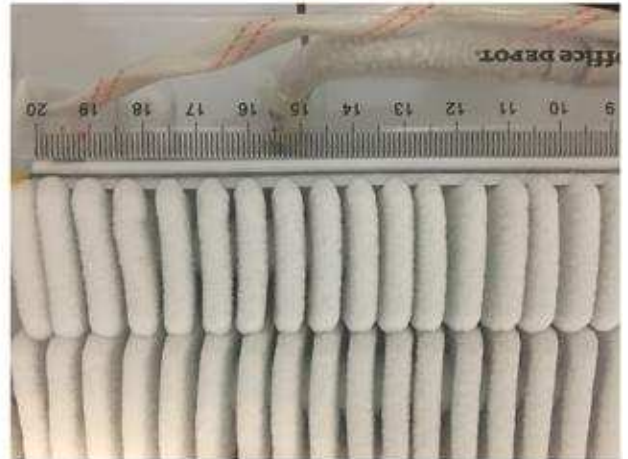
1



2



3



4



5



6

图 29. Frost Forming Process

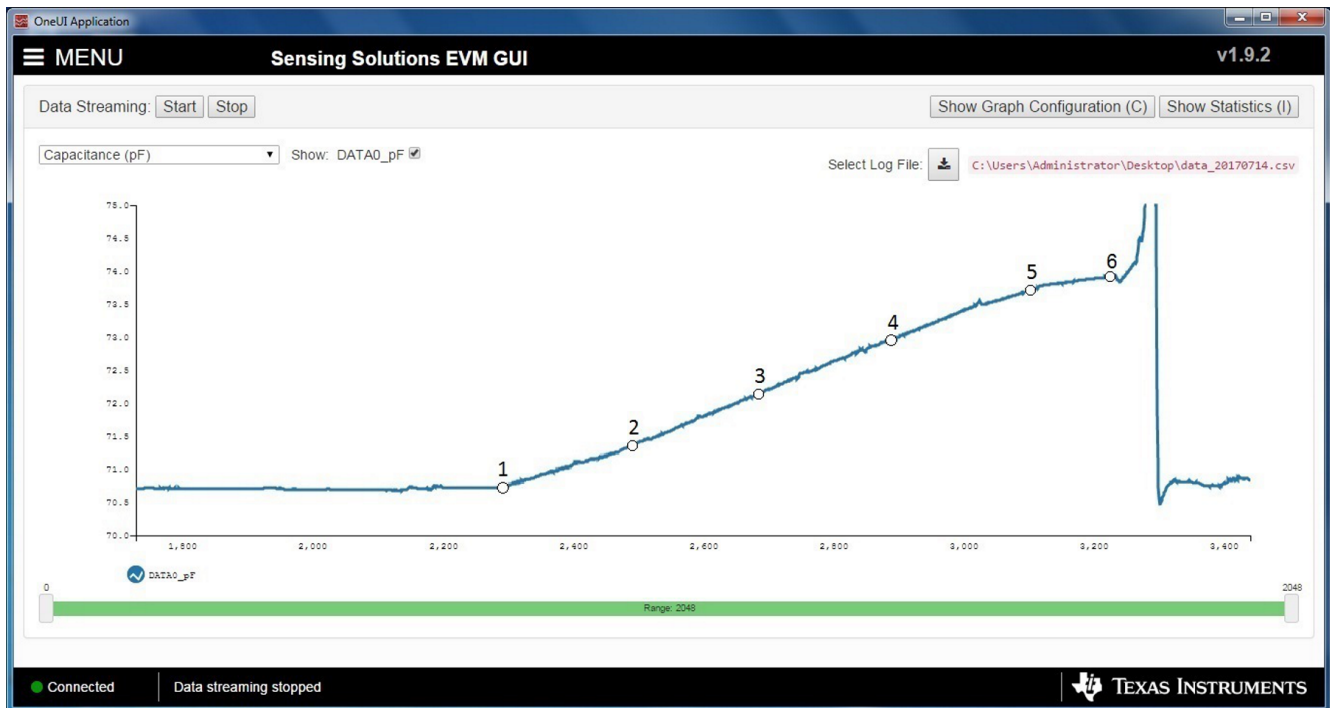


图 30. Sensed Capacitance During Frost Forming Process

4.2.3 Temperature Drift Test

The FDC2214 device uses an L-C tank as a sensor. The change in capacitance of the L-C tank is observed as a shift in the resonant frequency. The value stability of an onboard LC is significantly important to sense the external capacitance change. This test aims to verify the temperature drift of the board when the sensor is not connected. 图 31 shows the test setup.



图 31. Temperature Drift Test Setup

图 32 shows the comparison of temperature drift between the PCB coil and the common SMD inductor. The graph shows that use of a PCB coil is much more stable than an SMD inductor.

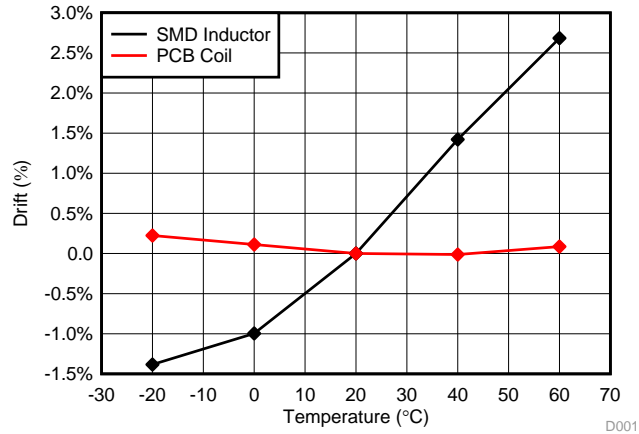


图 32. Capacitance Temperature Drift For PCB Coil and Common SMD Inductor

4.2.4 Environmental Susceptibility

Some common environmental interferences around the sensor area, such as a human moving nearby or a waterdrop, are always key concerns for capacitance sensing. This test simulates the worst-case scenario from when a finger touches the surface of the sensor and monitors the capacitance change (see 图 33).

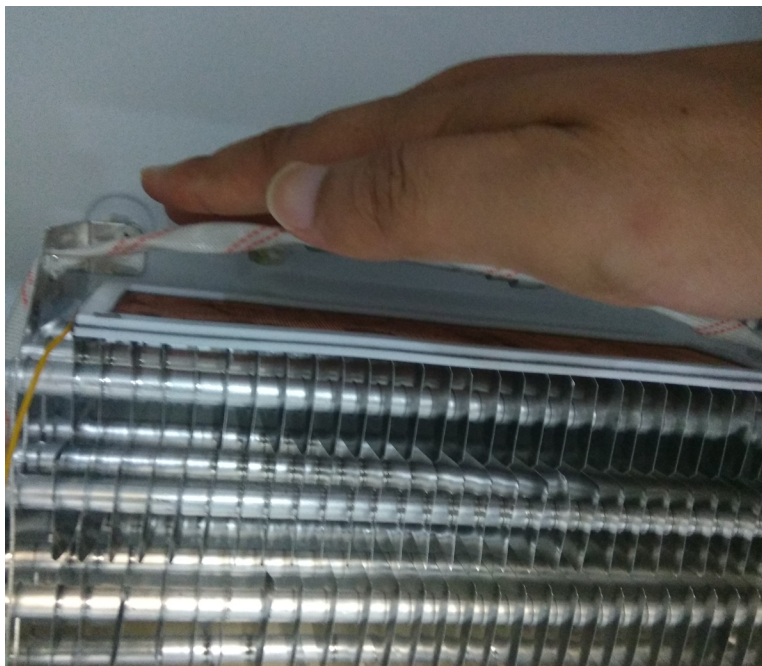


图 33. Sensor Touched By Finger

In this test, a hand is placed close to the top surface of sensor. The capacitance change registered is from 70.7 pF to 70.8 pF, which has a very negligible effect. This test aims to determine if there is any influence when a human body is in motion around the refrigerator. The results show that this influence is quite small and negligible for frost or ice detection.

Placement of a waterdrop on the surface of the sensor has also been tested (see 图 34) and the result shows that the value change is less than 0.1 pF.



图 34. Waterdrop on Surface of Sensor

4.2.5 Influence of Long Cable Connection

Cable lines pick up any parasitic capacitance and noise along the line, so the signal path distance between the sensor and FDC2114 must be as short as possible. This test uses a 1.5-m long cable to test the influence (see 图 35).



图 35. Long Cable Test Setup

As 图 36 shows, the baseline of capacitance increases from 70.7 pF to 100.5 pF due to cable parasitic capacitance, which is why TI recommends to use a short cable. However, the capacitance change curve remains the same as before.



图 36. Capacitance Curve in Single Cycle

4.2.6 Multi-Cycle Repeatability test

图 37 shows the capacitance for three cycles of frost formation and defrost. During the third cycle, the capacitance remains as a constant value because the thickness of frost has reached the limitation and touched the surface of the sensor, which is marked red. With this characteristic, the user can set the thickness limitation accordingly.

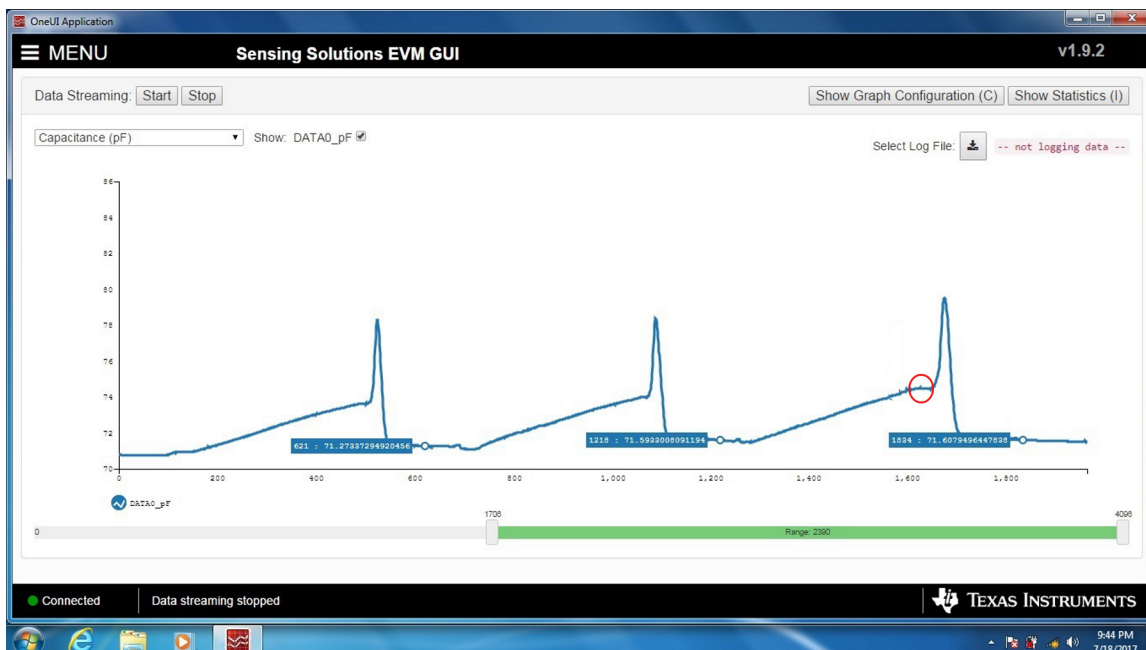


图 37. Capacitance Curve in Multi-Cycle Repeatability Test

5 Design Files

5.1 Schematics

To download the schematics, see the design files at [TIDA-01465](#).

5.2 Bill of Materials

To download the bill of materials (BOM), see the design files at [TIDA-01465](#).

5.3 PCB Layout Recommendations

- Avoid long traces to connect the sensor to the FDC. Short traces reduce parasitic capacitances between the sensor inductor and offer higher system performance.
- Systems that require matched channel response must have matched trace length on all active channels.

5.3.1 Layout Prints

To download the layer plots, see the design files at [TIDA-01465](#).

5.4 Altium Project

To download the Altium project files, see the design files at [TIDA-01465](#).

5.5 Gerber Files

To download the Gerber files, see the design files at [TIDA-01465](#).

5.6 Assembly Drawings

To download the assembly drawings, see the design files at [TIDA-01465](#).

6 Related Documentation

1. Texas Instruments, [FDC2x1x EMI-Resistant 28-Bit, 12-Bit Capacitance-to-Digital Converter for Proximity and Level Sensing Applications](#), FDC2214 Data Sheet, (SNOSCZ5)
2. Texas Instruments, [FDC2114 and FDC2214 EVM User's Guide](#), FDC2114/FDC2214 User's Guide (SNOU138)
3. Texas Instruments, [Proximity Sensing of up to 30-cm Range With >15-dB SNR and Robust Capacitive Touch Reference Design](#), TIDA-00474 Reference Design (TIDUUAU2)
4. Texas Instruments, [Backlight and Smart Lighting Control by Ambient Light and Proximity Sensor](#), TIDA-00754 Reference Design (TIDUB42)
5. Texas Instruments, [FDC1004: Basics of Capacitive Sensing and Applications](#), Application Report, (SNOA927)

6.1 商标

MSP430 is a trademark of Texas Instruments.
Microsoft, Windows are registered trademarks of Microsoft Corporation.
All other trademarks are the property of their respective owners.

7 About the Author

YICHANG (RICHARD) WANG is a Systems Architect at Texas Instruments, where he is responsible for developing reference design solutions for the industrial segment. Richard brings to this role his extensive experience in home appliances, including power electronics, high frequency DC-DC, AC-DC converter, analog circuit design and so on. Richard got his master's degree in Electrical Engineering and Automation from Nanjing University of Aeronautics and Astronautics, China.

有关 TI 设计信息和资源的重要通知

德州仪器 (TI) 公司提供的技术、应用或其他设计建议、服务或信息，包括但不限于与评估模块有关的参考设计和材料（总称“TI 资源”），旨在帮助设计人员开发整合了 TI 产品的应用；如果您（个人，或如果是代表贵公司，则为贵公司）以任何方式下载、访问或使用了任何特定的 TI 资源，即表示贵方同意仅为该等目标，按照本通知的条款进行使用。

TI 所提供的 TI 资源，并未扩大或以其他方式修改 TI 对 TI 产品的公开适用的质保及质保免责声明；也未导致 TI 承担任何额外的义务或责任。TI 有权对其 TI 资源进行纠正、增强、改进和其他修改。

您理解并同意，在设计应用时应自行实施独立的分析、评价和判断，且应全权负责并确保应用的安全性，以及您的应用（包括应用中使用的 TI 产品）应符合所有适用的法律法规及其他相关要求。您就您的应用声明，您具备制订和实施下列保障措施所需的一切必要专业知识，能够 (1) 预见故障的危险后果，(2) 监视故障及其后果，以及 (3) 降低可能导致危险的故障几率并采取适当措施。您同意，在使用或分发包含 TI 产品的任何应用前，您将彻底测试该等应用和该等应用所用 TI 产品的功能。除特定 TI 资源的公开文档中明确列出的测试外，TI 未进行任何其他测试。

您只有在为开发包含该等 TI 资源所列 TI 产品的应用时，才被授权使用、复制和修改任何相关单项 TI 资源。但并未依据禁止反言原则或其他法律授予您任何 TI 知识产权的任何其他明示或默示的许可，也未授予您 TI 或第三方的任何技术或知识产权的许可，该等产权包括但不限于任何专利权、版权、屏蔽作品权或与使用 TI 产品或服务的任何整合、机器制作、流程相关的其他知识产权。涉及或参考了第三方产品或服务的信息不构成使用此类产品或服务的许可或与其相关的保证或认可。使用 TI 资源可能需要您向第三方获得对该等第三方专利或其他知识产权的许可。

TI 资源系“按原样”提供。TI 兹免除对 TI 资源及其使用作出所有其他明确或默认的保证或陈述，包括但不限于对准确性或完整性、产权保证、无复发故障保证，以及适销性、适合特定用途和不侵犯任何第三方知识产权的任何默认保证。

TI 不负责任何申索，包括但不限于因组合产品所致或与之有关的申索，也不为您辩护或赔偿，即使该等产品组合已列于 TI 资源或其他地方。对因 TI 资源或其使用引起或与之有关的任何实际的、直接的、特殊的、附带的、间接的、惩罚性的、偶发的、从属或惩戒性损害赔偿，不管 TI 是否获悉可能会产生上述损害赔偿，TI 概不负责。

您同意向 TI 及其代表全额赔偿因您不遵守本通知条款和条件而引起的任何损害、费用、损失和/或责任。

本通知适用于 TI 资源。另有其他条款适用于某些类型的材料、TI 产品和服务的使用和采购。这些条款包括但不限于适用于 TI 的半导体产品 (<http://www.ti.com/sc/docs/stdterms.htm>)、[评估模块](http://www.ti.com/sc/docs/sampters.htm)和样品 (<http://www.ti.com/sc/docs/sampters.htm>) 的标准条款。

邮寄地址：上海市浦东新区世纪大道 1568 号中建大厦 32 楼，邮政编码：200122
Copyright © 2017 德州仪器半导体技术（上海）有限公司